Deterministic properties of mine tremor aftershocks

T.E. Kgarume *CSIR Centre for Mining Innovation and University of the Witwatersrand, South Africa*

S.M. Spottiswoode *Consultant, South Africa*

R.J. Durrheim *CSIR Centre for Mining Innovation and University of the Witwatersrand, South Africa*

Abstract

Mine tremor aftershock sequences from two deep mines in the Far West Rand goldfield, South Africa, were analysed in order to determine the influence of geological and mining parameters on the risk posed by aftershocks. Mainshocks were stacked in time and space and the aftershock productivity was calculated for various subsets. Contrary to our working hypothesis, no significant differences were found between the aftershock productivity of mainshocks located in high stress areas and those located in low stress areas, or between mainshocks located in high strain-rate areas and those located in low strain-rate areas, or between mainshocks located near to geological features and those located further away from geological features. Thus, while the incidence of mainshocks may be affected by stress, strain rate and proximity of geological features, these factors do not have significant influence on aftershock productivity. Consequently, guidelines governing the time period and distance from the mainshock in which hazard is considered to be elevated need not take variations in these geological and mining parameters into account.

1 Introduction

The importance of understanding the changes in hazard following larger mining-related seismic events was highlighted by a M2.4 seismic event that occurred in a deep South African gold mine in October 2006, causing severe damage to a stope and fatally injuring several mine workers. An M2.0 event had occurred nearby 25 minutes prior to the M2.4 event, but miners were not evacuated from working places as the event did not cause any damage. However, the question arose whether the M2.0 event might have triggered, in some way, the M2.4 event. Members of the ‘‘Minimising the rockburst risk’’ research team were directed by the Chief Inspector of Mines to investigate changes in seismic hazard following the occurrence of large seismic events, and to formulate guidelines governing the evacuation of workers following such events. The results of the statistical analysis were reported by Kgarume et al. (2010). The factors driving seismicity in mines (e.g. proximity of geological weaknesses, geometry of the excavations, sequence and rate of mining) are quantifiable and, to some extent, controllable. This study seeks to determine the influence of these of geological and mining parameters on the hazard posed by aftershocks.

“Aftershock productivity” refers to the rate and density of aftershocks succeeding the mainshock. Investigations of aftershock sequences have shown that productivity is a function of the mainshock magnitude (Felzer et. al., 2004):

$$n = n_0 10^{\alpha M_M} \tag{1}$$

Where:

n = number of aftershocks

n_0 = productivity constant

α = parameter that controls the relative number of aftershocks as a function of the mainshock magnitude

M_M = magnitude of the triggering mainshock. The magnitude scale commonly used in South African mines is based on a combination of moment and energy measurements, and approximates the local magnitude scale.

Using the southern California catalogue, Felzer et al. (2004) determined a value of 1.0 for α by counting the number of triggered earthquakes as a function of the triggering mainshock magnitude, while Helmstetter et al. (2005) obtained a similar value of 1.05 by stacking aftershock sequences which have the same triggering mainshock magnitude. The value of α, particularly when $\alpha \approx b$ (where b is the b-value of the sequence), was interpreted to indicate that small earthquakes are roughly as important to earthquake triggering as larger ones (Helmstetter et al., 2005).

Aftershock sequences have been studied to elucidate various aspects of the physics of the Earth. For example, a study of deep crustal earthquakes found that aftershock productivity was a function of the depth of the mainshock, and abrupt changes in aftershock productivity at certain mainshock depths were interpreted to be the result of changes in earthquake generation and rupture mechanisms (Persh and Houston, 2004). Yang and Ben-Zion (2009) found that aftershock productivity has an inverse relationship with the mean heat flow.

2 Deterministic analysis of mine tremor aftershocks

2.1 Mining parameters

The incidence of mining-tremors is often controlled by stress, strain rate, and proximity to geological features. To investigate whether aftershock productivity is also affected by these parameters, the mainshocks were divided into two populations based on the median value of the parameter under consideration. Data from two gold mines in the Far West Rand mining district, where mining takes place at depths reaching 3500 m below the surface, were used to investigate the aftershock productivity (Table 1). The reefs being mined are the Carbon Leader reef (CLR) and the Ventersdorp Contact reef (VCR). (Note that the term ‘‘reef’’ denotes a quartz pebble conglomerate.) The terminology used to describe stopes in South African mines is shown in Figure 1.

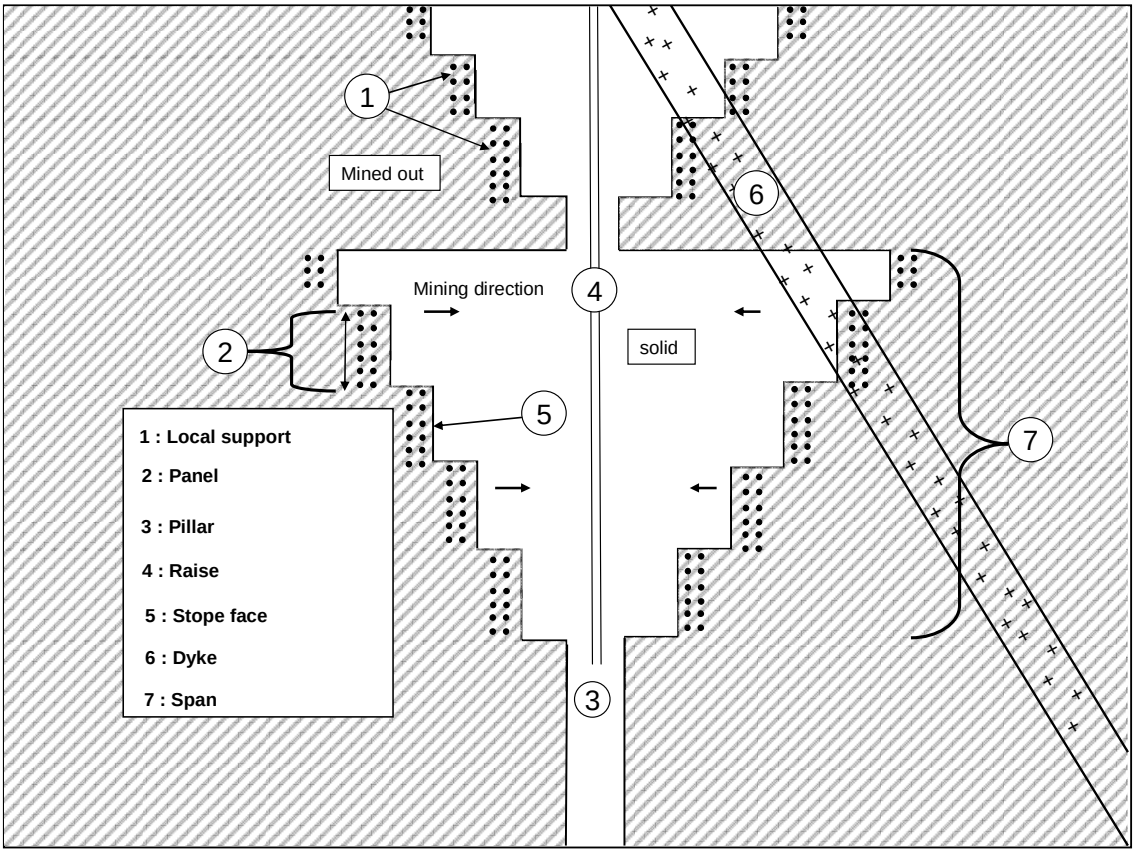

Figure 1 Simplified mine plan showing the main elements of stopes in South African gold mines

Table 1 Datasets used in the analysis

	Magnitude range		
Ore body		VCR	CLR
Start of catalogue		01/01/2003	02/01/1998
End of catalogue		09/11/2007	08/01/2007
Blasting time		17h00 – 21h00	12h00 – 18h00
No. events in catalogue	$0.0 \leq M \leq 4.0$	5155	10169
Mainshocks	$2.0 \leq M \leq 4.0$	94	390
Aftershocks	$0.0 \leq M$	5061	9785
Maximum time for aftershocks		1 week	1 week
Maximum distance of aftershocks (m)		1000	1000
ERR, median value (MJ/m^2)		9.4	10.6
Distance to face, median value (m)		46.3	26.1
Distance to geological discontinuities, median value (m)		51.0	43.0

2.3 Methodology

The Modified Omori law (equation 2), which describes the decay of aftershocks with time following the mainshock (Nanjo et al., 1998), was used to determine the aftershock productivity

$$n(t) = \frac{K}{(t+c)^p} \tag{2}$$

Where:

t = time after the mainshock

$n(t)$ = number of events occurring at time t

K = aftershock productivity

c = 'time offset' parameter

p = rate constant of aftershock decay, with $p \approx 1$ for natural earthquakes and $0.6 \leq p \leq 1.03$ for mine tremor aftershock and foreshock sequences (Spottiswoode, 2000; Kgarume et al., 2010).

The productivity K was determined by integrating equation (2), assuming p=1:

$$N(t) = K[\ln(t+c) - \ln(t_0 + c)] \tag{3}$$

Where:

$N(t)$ = cumulated number of aftershocks

t_0 = initial time of the sequence

K = aftershock productivity, determined in practice by the slope of $N(t)$ versus log (t)

In order to increase the number of aftershocks in a sample and hence the robustness of the statistical analysis, the mainshocks within a particular population were aligned in space and time and the succeeded seismicity

stacked in time and space windows (Kgarume et al., 2010). In this study, all seismic events occurring within 1000 m of the mainshock were stacked, cumulated over a period of seven days, and then normalised by the number of mainshocks. The "total" seismicity (curve labelled "cumulative data" in Figure 2) includes the aftershocks as well as "background" activity seismicity generated by routine mining activity. "Background" seismicity was estimated by averaging the seismicity recorded during three week-long windows, starting one week after the mainshock and including seismicity recorded within the blasting periods. The background seismicity dominates the aftershock activity and becomes exponential at later times due to its constant behaviour on a linear scale. To take this into account, a "background" term βt was added to equation (3) to give:

$$N(t) = K[\ln(t + c) - \ln(t_0 + c)] + \beta t \tag{4}$$

Aftershock productivity was estimated by subtracting the "background" curve from the "total" curve to yield an estimate of the aftershocks. The slope of this de-trended curve provides an estimate of *K*.

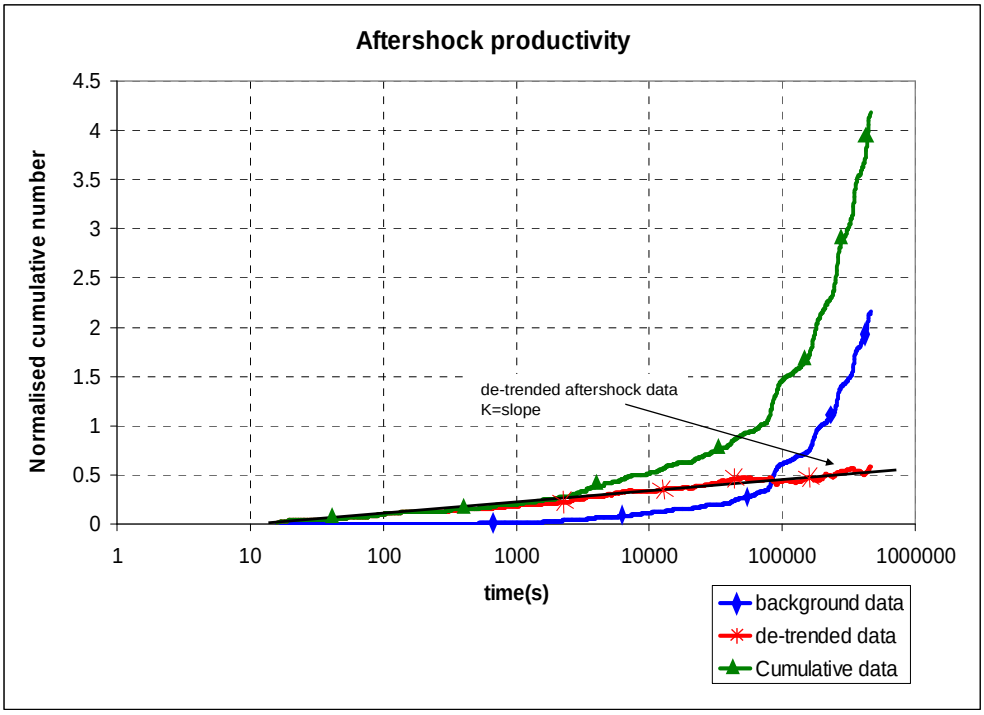

Figure 2 Estimate of aftershock productivity after M ≥ 2.0 mainshocks.

All events with M ≥ 2.0 occurring outside blasting time were classified as mainshocks. (Mainshocks that occurring during blasting time were excluded from the analysis, as seismic activity is swamped by the blasting-induced seismicity and the recording sensitivity of the system degraded.) Aftershocks were classified as all events with $0.0 \leq M \leq M_M$ that occurred within 1 week and 1000 m of the mainshock, including events that occurred during blasting time. Blasting activity significantly increases the number of recorded events, but this effect is corrected for when the data is de-trended.

For each geological and mining parameter, mainshocks were divided into two equal populations based on the median value of the parameter (Table 1). For example, to study the influence of stress on aftershock productivity, mainshocks located in high stress environments (e.g. abutments and pillars) were separated from those located in relatively low stress environments (Figure 3A). Similarly, mainshocks located in high strain-rate environments (areas of active mining) were separated from those located in low strain-rate environments (areas without active mining) (Figure 3B), and mainshocks located in close proximity to geological features (dykes and faults) were separated from those located further away from the features (Figure 3C). Figure 4 demonstrates the mainshock division. Population 1 represents mainshocks locating close to geological features and population 2 represents mainshocks locating further away from geological features.

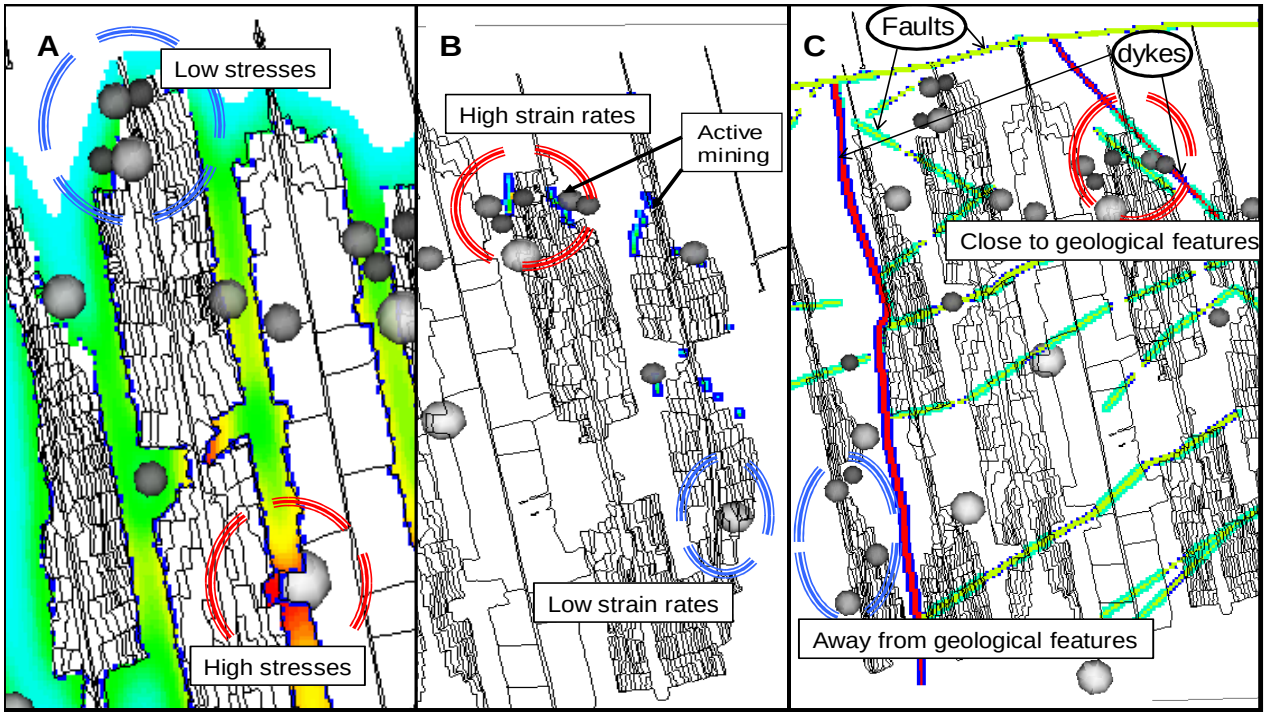

Figure 3 **Mine plans illustrating the parameters used to define mining conditions. (A) Stress, (B) Strain rate, and (C) Geological discontinuities. Lines indicate face positions and spheres indicate seismic events.**

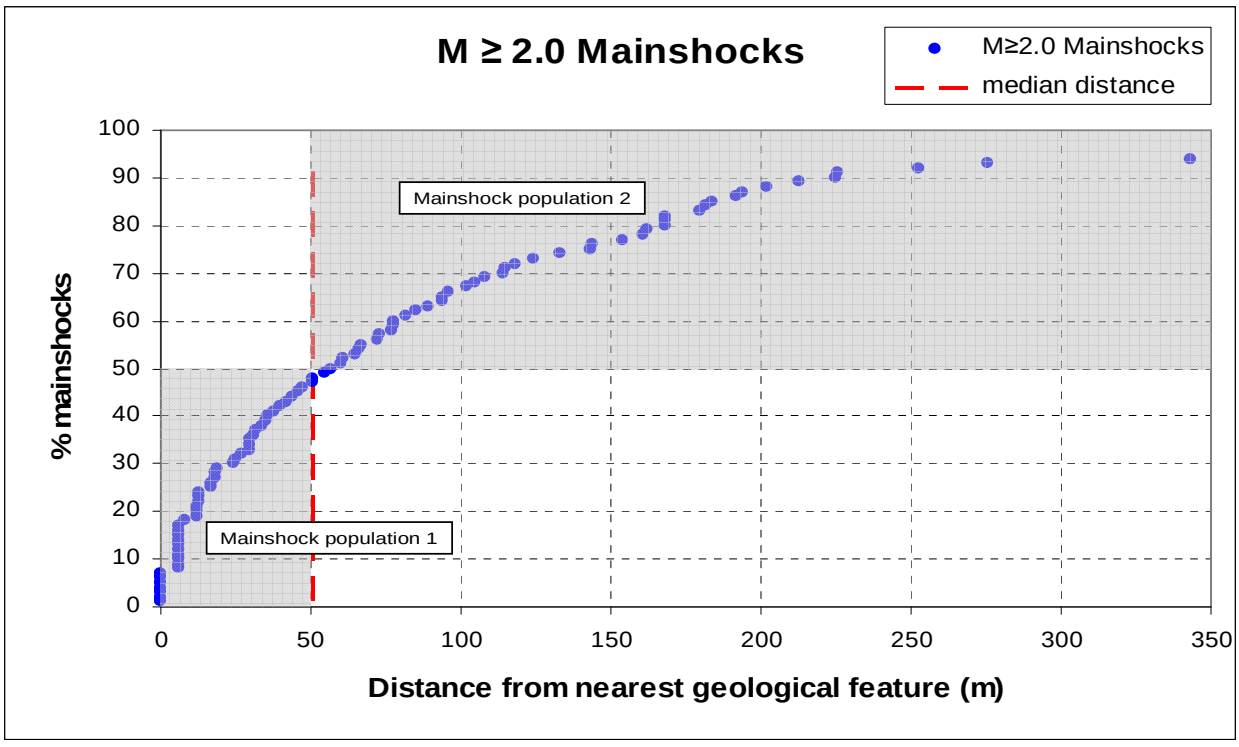

Figure 4 **Division of mainshocks into two populations to study the influence of geological discontinuity on aftershock productivity. The median distance of mainshocks from geological features is used to define the two mainshock populations.**

4 Findings

4.1 Effect of geological and mining parameters on aftershock productivity

As mining progresses, the extraction of rock causes stress to be redistributed from mined-out to unmined ground. High stress concentrations may be created, particularly in pillars and immediately ahead of stope faces. In this study we used the Energy Release Rate (*ERR*) as a proxy for stress. *ERR* is a measure of energy changes and stress concentration at the stope face related to the extent of volumetric convergence taking place in the back area of the stope (Jager and Ryder, 1999, p.46). *ERR* is defined as:

$$ERR = \frac{1}{2} q_v \, \Delta V \Big/ \Delta A \ \text{MJ/m}^2 \tag{5}$$

Where:

q_v = virgin vertical stress

ΔA = extracted area

ΔV = volume change due to stope closure.

High *ERR* correlates with stresses in front of the face, shear stresses on planes of weaknesses, and the depth and height of fracturing (Jager and Ryder, 1999, p. 49). Using data from the VCR and CLR mines, Spottiswoode et al. (2008) showed that *ERR* is, on average, a good measure of likely seismicity. However, *ERR* has its limitations as an estimator of seismicity as it does not take the presence of geological discontinuities into account, which may be associated with increased levels of seismicity. The VCR and CLR mainshock populations were divided into high- and low-stress subsets based on the median ERR value of 10.6 MJ/m^2 and 9.4 MJ/m^2, respectively. However, the high and low *ERR* populations were found to have similar levels of aftershock productivity.

Mainshocks located in close proximity to actively mined faces are in a high strain-rate environment, while those located further away from actively mined faces or close to faces that are not being mined are in a relatively low strain-rate environment. To investigate the influence of strain rate, the distance (D) to actively mined faces was used as a proxy for strain rate. Figure 6 compares aftershock sequences following mainshocks located in high strain-rate and low strain-rate environments. The VCR and CLR mainshock populations were divided into high and low strain-rate subsets based on the median distance to actively mined faces of 46.3 m and 26.1 m, respectively. However, the high and low strain-rate populations were found to have similar levels of aftershock productivity. A similar analysis was conducted to investigate the relationship between aftershock productivity and the proximity to geological features (Figure 7). Again, on both the VCR or CLR mines, a similar value was found for the populations near to or far from geological structures. To investigate whether the differences between the productivity of the populations are statistically significant, we computed the confidence intervals associated with the least-squares estimate of the productivity K.

The confidence interval of least-squares estimate of productivity $\hat{K}$ is given by:

$$[\hat{K} - s_{\hat{K}} T_{n-2}, \hat{K} + s_{\hat{K}} T_{n-2}] \tag{6}$$

Where:

$s_{\hat{K}}$ = standard deviation of $\hat{K}$

n = number of aftershocks

T_{n-2} = Student's t-values with n-2 degrees of freedom

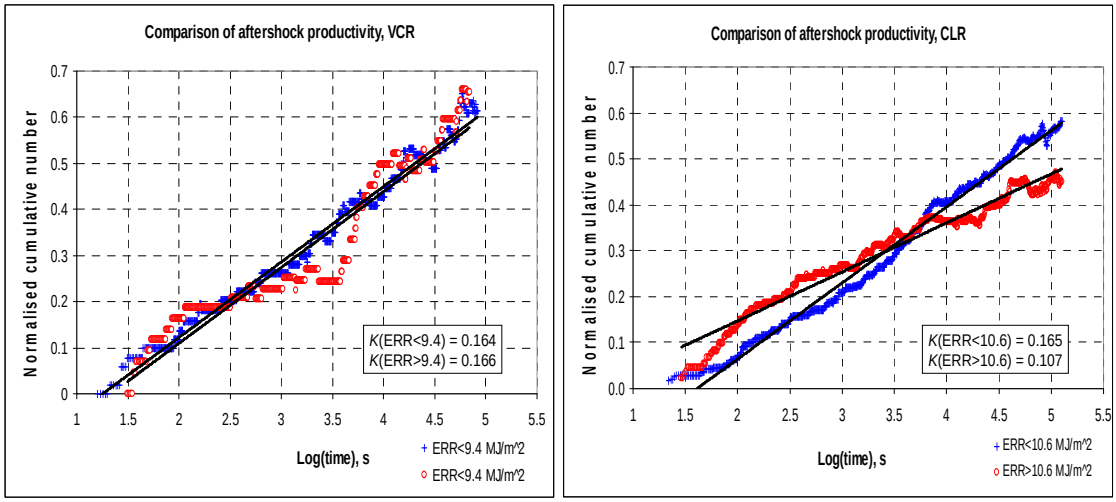

Figure 5 Effect of stress environment on aftershock productivity

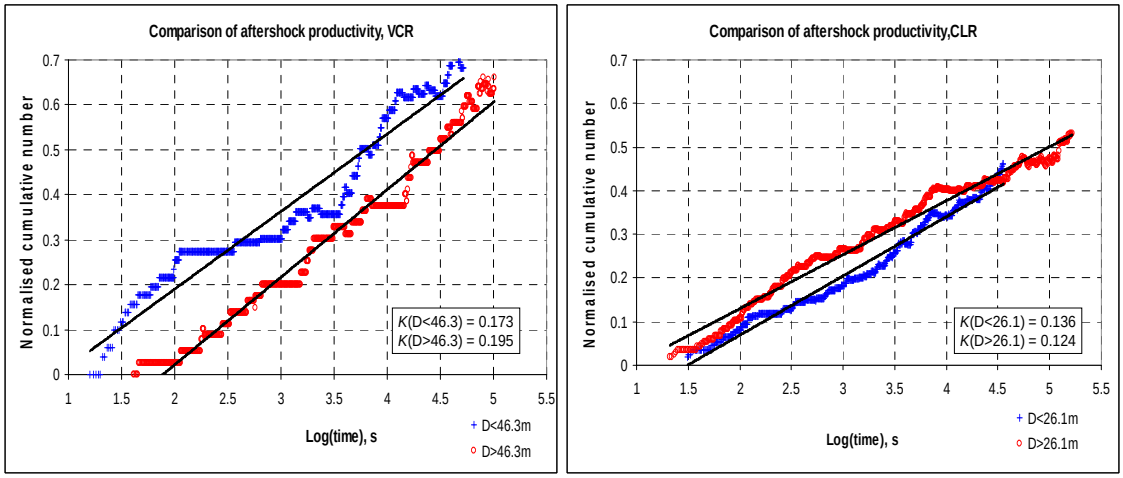

Figure 6 Effect of strain rate on aftershock productivity

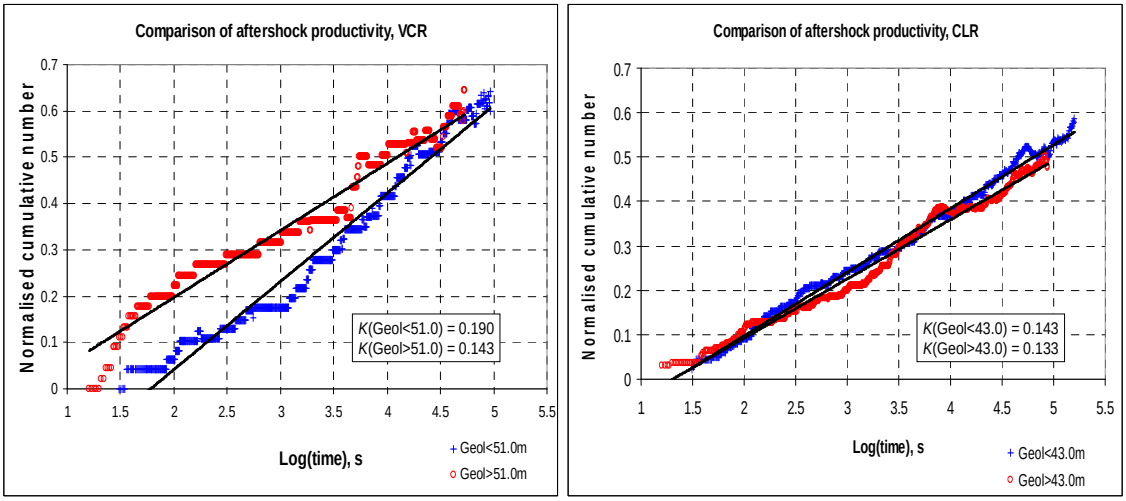

Figure 7 Effect of proximity to geological features on aftershock productivity

The standard deviation of $\hat{K}$ is given by

$$s_{\hat{K}} = \sqrt{\frac{\frac{1}{n-2}\sum_{i=1}^{n} \varepsilon_i^2}{\sum_{i=1}^{n}\left(x_i - \bar{x}\right)^2}} \tag{7}$$

where:

x_i = time of occurrence of aftershocks

$\bar{x}$ = mean time of occurrence of aftershocks

ε_i^2 = square of the residuals of the normalized cumulated aftershocks

The table below summarizes the results of the comparisons. The confidence intervals of the slopes are computed at the 95% confidence level.

Table 2 Statistical comparison of aftershock productivity for contrasting mining parameters

Orebody	VCR		CLR	
	95% confidence interval of K		95% confidence interval of K	
ERR (MJ/m^2)	< 9.4	$0.163 \leq 0.164 \leq 0.165$	< 10.6	$0.164 \leq 0.165 \leq 0.166$
	> 9.4	$0.154 \leq 0.158 \leq 0.162$	> 10.6	$0.106 \leq 0.107 \leq 0.108$
Geol (m)	< 51.0	$0.188 \leq 0.190 \leq 0.192$	< 43.0	$0.142 \leq 0.143 \leq 0.144$
	> 51.0	$0.143 \leq 0.145 \leq 0.147$	> 43.0	$0.132 \leq 0.133 \leq 0.134$
D (m)	< 46.3	$0.170 \leq 0.173 \leq 0.176$	< 26.1	$0.135 \leq 0.136 \leq 0.137$
	> 46.3	$0.193 \leq 0.195 \leq 0.197$	> 26.1	$0.123 \leq 0.124 \leq 0.125$

A significant difference in the aftershock productivity is found when comparing the two contrasting mining parameters at the 95% confidence level. Productivity of mainshocks locating in environments with values less than the median of the parameter tend to have a significantly higher slope. The only exception is the comparison between the slopes of the strain environments at the VCR where the slope is higher for mainshocks locating further away from actively mined faces.

4.2 Effect of mainshock magnitude on aftershock productivity

To investigate the dependency of aftershock productivity on the magnitude of the triggering mainshock, aftershock sequences within 1 hour and 400 metres of the mainshock were stacked. A time period of 1 hour ensures that the aftershock productivity is not unduly contaminated by background seismicity, while 400 metres is the typical dimension of a stope in a South African mine. Mainshock magnitude M_M ranged from M_M = 1.0 – 3.0. M ≥ 0.0 aftershocks were cumulated with time and normalised to the number of stacked mainshocks. Aftershock productivity *K* was determined as a function of the triggering mainshock magnitude for each mainshock class M_M to (M_M + ΔM). A bin size of ΔM = 0.5 was used. Due to small sample statistics, the productivity data-point for the M_M = 3.0 - 3.5 bin was omitted from the VCR data set. Table 3 summarises the results. Figure 8 shows the relationship between aftershock productivity and the mainshock magnitude. The parameter α is given by the slope of the regression line.

The productivity *K* of aftershocks with magnitude M ≥ M_{min} (where M_{min} = 0.0) triggered by a mainshock of magnitude M_M increases with M_M as $K = K_0 10^{\alpha M_M}$ where α = 1.33 ± 0.10 and 0.88 ± 0.11 for the VCR and CLR reefs, respectively. The standard deviations are constructed at the 95% confidence level. These values

are similar to the values of 1.0 and 1.05 obtained by Felzer et al. (2004) and Helmstetter et al. (2005), respectively.

Table 3 Aftershock productivity *K* as a function of the mainshock magnitude

VCR			
M_M bins	**$N(M_M)$**	***K***	**$Log(K/N(M_M))$**
1.0 – 1.5	329	0.056	-3.76
1.5 – 2.0	145	0.076	-3.27
2.0 – 2.5	36	0.112	-2.5
2.5 – 3.0	12	0.19	-1.8
3.0 – 3.5	-	-	-
CLR			
1.0 – 1.5	839	0.133	-3.79
1.5 – 2.0	475	0.120	-3.59
2.0 – 2.5	159	0.156	-3.00
2.5 – 3.0	58	0.177	-2.51
3.0 – 3.5	13	0.097	-2.12

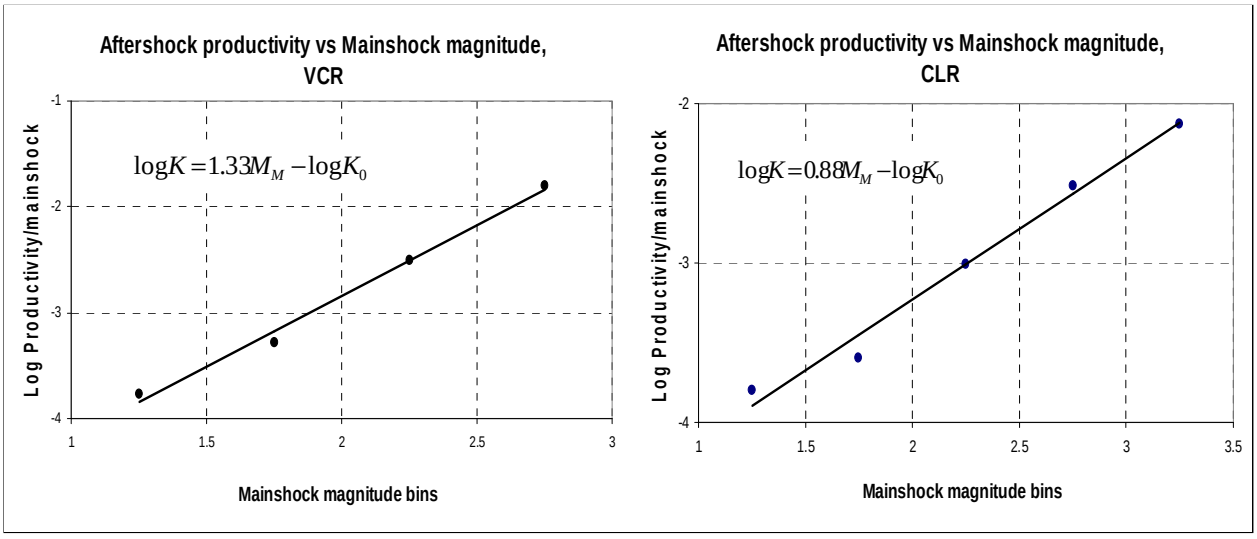

Figure 8 Aftershock productivity *K* as a function of the mainshock magnitude

4.3 Aftershock hazard

The goal of this study was to derive guidelines to govern the exposure of workers to elevated seismic hazard following a larger seismic event. By way of example, two hazard thresholds were used: 3× and 10× the background rates of seismicity (Figure 9). Of course, aftershocks will continue to occur even after the activity declines below these thresholds.

The question arises, what proportion of the events in the catalogue are aftershocks occurring in these relatively high hazard times? The ratio was computed by determining the number of aftershocks which occurred within 200 m of the mainshock and during times when the event rate exceeded 3× and 10× the background rate limits defined by the aftershock decay curve (Figure 9).

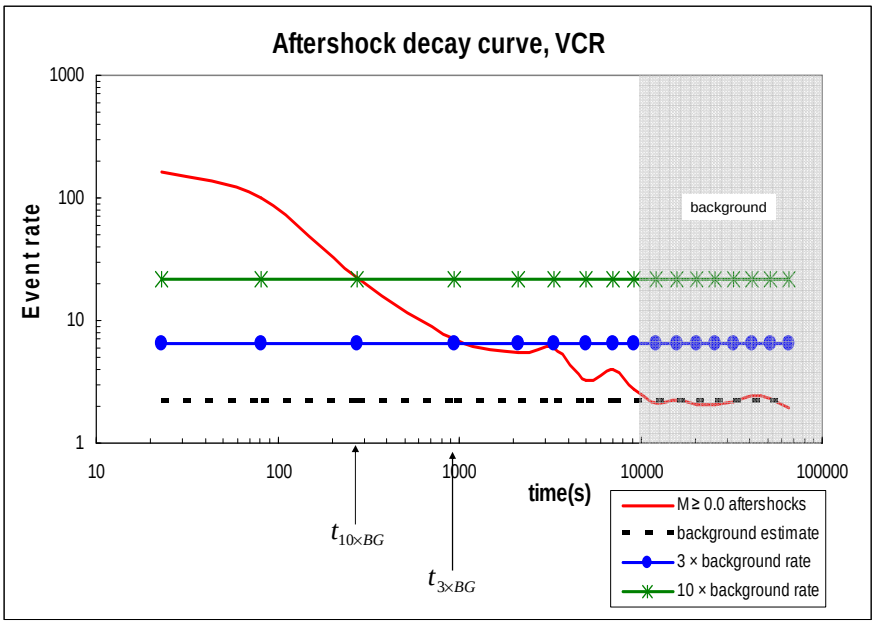

Figure 9 Number of M ≥ 0.0 aftershocks within 200 m of $2.0 \leq M_M \leq 3.0$ mainshocks. The curve was used to determine the number of aftershocks that occurred while activity exceeded 3× and 10× the background rate.

Equation 5 was used to determine the aftershock proportion.

$$P = \frac{N_A(t_0, t_{A\_\max})}{N_{Total}(t_0, t_{\max})} \quad (5)$$

Where:

t_0 = source duration (1 second)

t_{A_max} = time taken for aftershock decay rate to reach 3× and 10× the background rate.

N_A = number of aftershocks occurring within t_0 and t_{A_max} during an 8-hour working shift (excludes seismicity occurring within the blasting period).

t_{max} = long time period, when mining would have extended into or past the source region

N_{total} = total number of seismic events occurring within an 8-hour working shift (excludes seismicity occurring within the blasting period).

Table 4 gives the proportion of aftershocks within the working shift with reference to the 3× and 10× the background rates. Table 3 shows that for $2.0 \leq M_M \leq 4.0$ mainshocks, the aftershocks that occur while the rate of seismicity is 3× higher than the background rate represent about 52% and 46% of the events recorded during the working shift on the VCR and CLR mines, respectively. This suggests that exposure to a significant proportion of potentially damaging events could be avoided by evacuating working places for a period of time following the occurrence of mainshocks exceeding M2.0.

Table 4 Proportion of aftershocks within the working shift and 200 m of the mainshock epicentre.

	VCR $N_{main} = 42$	**CLR** $N_{main} = 228$
$2.0 \leq M_M \leq 4.0$	**Proportion of aftershocks (%)**	**Proportion of aftershocks (%)**
3 × BG	52.1	46.2
10 × BG	41.5	41.6

5 Conclusions

Previous studies have indicated that the incidence of mining-related tremors in deep South African gold mines are often affected by stress, strain rate, and the proximity of mining to geological features. This study of mine tremor aftershock sequences from two Far West Rand gold mines was undertaken to determine if these factors also affect aftershock productivity, and hence the seismic hazard following larger seismic events. The main findings were:

- The productivity of mine tremor aftershocks showed a $10^{\alpha M_M}$ dependency on the magnitude of the triggering mainshock, where α has a value close to 1, i.e. an increase of one magnitude unit on mainshock size results in a 10-fold increase in the number of aftershocks. This is similar to the relationship obtained for tectonic earthquakes in southern California.
- About half the M>0.0 events that occurred during shift times were aftershocks of M>2.0 events, and occurred during the few minutes to tens of minutes that it took for the hazard level to subside to three times the background level following these larger events. This suggests that exposure to a significant proportion of potentially damaging events could be avoided by evacuating nearby working places for a relatively short period of time following the occurrence of mainshocks with M>2.0.
- No major influence of stress, strain rate, and the proximity of mining to geological features on aftershock productivity was found. Consequently, guidelines governing the time and distance from the mainshock in which hazard is considered to be elevated need not take variations in these mining and geological parameters into account.

Acknowledgements

This study was supported by a CSIR studentship grant. The initial stage of the study was supported by the Mine Health and Safety Council through project SIM 050302 ‘‘Minimising the rockburst risk’’. Mine management is thanked for providing the seismic datasets used in the analysis.

References

Felzer, K. R. Abercrombie, R. E., and Ekstrom, G. (2004) A common origin for aftershocks, foreshocks, and multiplets, Bulletin of the Seismological Society of America, 94, pp. 88-99.

Helmstetter, A., Kagan, Y.Y. and Jackson, D.D. (2005) Importance of small earthquakes for stress transfers and earthquake triggering, Journal of Geophysical Research, 110, 2005, B05S08, doi: 10.1029/2004JB003286.

Jager, A. J. and Ryder, J. A. (1999) A Handbook on Rock Engineering Practice for Tabular Hard Rock Mines, Braamfontein: SIMRAC, 371 pp.

Kgarume, T., Spottiswoode, S. M. and Durrheim, R. J. (2010) Statistical properties of mine tremor aftershocks, Pure and Applied Geophysics, 167, pp. 107-117.

Nanjo, K., Nagahama, H. and Satomura, M. (1998) Rates of aftershock decay and the fractal structure of active fault systems, Tectonophysics, 287, pp. 173–186.

Persh, S. and Houston, H. (2004) Strongly depth-dependent aftershock production in deep earthquakes, Bulletin of the Seismological Society of America, 94, pp. 1808 - 1816.

Spottiswoode, S. M. (2000) Aftershocks and foreshocks of mine seismic events, 3rd International Workshop on the Application of Geophysics to Rock and Soil Engineering, GeoEng2000, Melbourne Australia.

Spottiswoode, S. M., Linzer, L. M. and Majiet, S. (2008) Energy and stiffness of mine models and seismicity, Proceedings of the First Southern Hemisphere International Rock Mechanics Symposium, Y. Potvin, J. Carter and R. Jeffrey (eds), Perth, Australia, September 2008, pp. 693 - 707.

Yang, W. and Ben-Zion, Y. (2009) Observational analysis of correlations between aftershock productivities and regional conditions in the context of a damage rheology model, Geophysical Journal International, 177, pp. 481-490.